

Chapter 2

Modelling of Structural Pounding

Modelling of earthquake-induced pounding between buildings, or bridge segments, requires the use of accurate structural models as well as appropriate models of the effects of collisions. Two different approaches can be found in the literature, which are usually used to simulate structural pounding during ground motions. The first approach considers the classical theory of impact, which is based on the laws of conservation of energy and momentum and does not consider stresses and deformations in the colliding structural elements during impact. Since this is not a force-based approach, the effect of collisions is accounted through updating the velocities of the considered bodies or structural elements. In the second approach, the earthquake-induced structural pounding is simulated using the direct model of impact force during collision.

2.1 Classical Theory of Impact

The classical theory of impact, called stereomechanics, is focuses on determination of velocities of colliding elements after collision without tracing structural response during impact (Goldsmith 1960). The analysis is based on the values of velocities of structural elements before collision with the use of the coefficient of restitution, which accounts for the energy dissipation during impact due to such effects as, for example, plastic deformations, local cracking and friction (see Leibovich et al. 1996; Ruangrassamee and Kawashima 2001; DesRoches and Muthukumar 2002). The formulae for the final (after impact) velocities \dot{x}_1^f, \dot{x}_2^f of two colliding elements with masses m_1 and m_2 (see Fig. 2.1) can be expressed as (Goldsmith 1960):

$$\dot{x}_1^f = \dot{x}_1^0 - (1 + e) \frac{m_2 \dot{x}_1^0 - m_2 \dot{x}_2^0}{m_1 + m_2} \quad (2.1a)$$

$$\dot{x}_2^f = \dot{x}_2^0 + (1 + e) \frac{m_1 \dot{x}_1^0 - m_1 \dot{x}_2^0}{m_1 + m_2} \quad (2.1b)$$

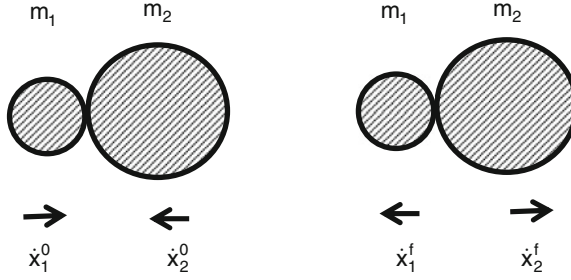


Fig. 2.1 Initial (before impact) and final (after impact) velocities of colliding bodies

where \dot{x}_1^0, \dot{x}_2^0 are the initial (before impact) velocities and e is a coefficient of restitution, which can be obtained from the equation:

$$e = \frac{\dot{x}_2^f - \dot{x}_1^f}{\dot{x}_1^0 - \dot{x}_2^0} \quad (2.2)$$

The value of $e = 1$ is related to the case of a fully elastic collision, while the value of $e = 0$ deals with a fully plastic impact. The basic value of the coefficient of restitution can be determined experimentally by dropping a sphere, made of the specific material, on a massive plane plate of the same material from a height h . Then, after recording the rebound height h^* , the following formula can be used (see Goldsmith 1960):

$$e^2 = \frac{h^*}{h} \quad (2.3)$$

It has been confirmed through experimental studies that the value of the coefficient of restitution usually ranges from 0.4 up to about 0.8 in the case of collisions between structural elements made of building materials (see Anagnostopoulos and Spiliopoulos 1992; Zhu et al. 2002; Jankowski 2010). Azevedo and Bento (1996) suggested that $e = 0.65$ should be used for typical concrete structures. In fact, this value has been used by a number of researchers in the analyses of pounding between different types of structures (see, for example, Anagnostopoulos 1988; Papadrakakis et al. 1991; Anagnostopoulos and Spiliopoulos 1992; Jankowski et al. 1998; Jankowski 2006b, 2008; Mahmoud et al. 2013). However, the results of the impact experiments indicate that the value of the coefficient of restitution might substantially depend on the prior-impact velocity as well as on the material of colliding elements (Jankowski 2010). The general trend for the typical building materials, such as: steel, concrete, timber and ceramic, shows a decrease in the coefficient of restitution as the prior impact velocity increases (see Fig. 2.2).

The value of the coefficient of restitution for colliding elements made of two different materials can be determined from the following formula (Goldsmith 1960):

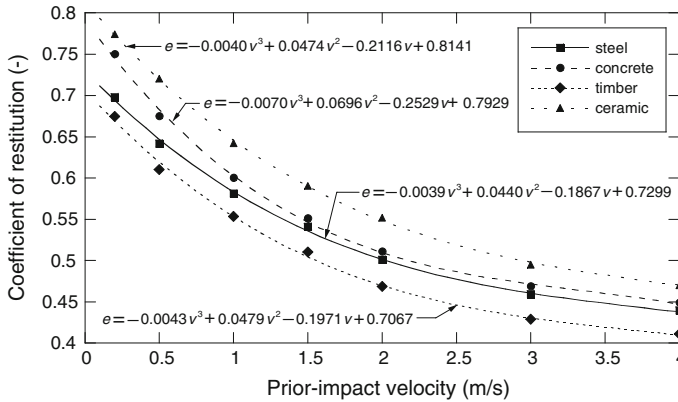


Fig. 2.2 Coefficient of restitution with respect to the prior-impact velocity (Jankowski 2010)

$$e = \frac{e_1 E_2 + e_2 E_1}{E_1 + E_2} \quad (2.4)$$

where e_i , E_i are the coefficient of restitution and modulus of elasticity for material i ($i = 1, 2$), respectively.

The use of the classical theory of impact is recommended for predicting the global effects on colliding bodies (Goldsmith 1960). However, its use in the analysis of earthquake-induced structural pounding is actually limited to the cases of collisions between only two structures which are modelled as lumped mass single-degree-of-freedom (SDOF) systems (see, for example, Ruangrassamee and Kawashima 2001). This limitation results from the fact that the approach does not consider stresses and deformations in the colliding structural elements during impact (it is assumed that contact lasts negligibly short time) and the behaviour of structures during impact is not obtained. Therefore, the approach is not recommended when structures are modelled as multi-degree-of freedom systems or when the study on pounding of buildings in series, or between several segments of a bridge, is conducted. In such cases, the structural response during the whole time of contact is important, since collision between other structural elements might take place at the same time. It is also possible that when two structural elements rebound after collision they might come into contact with other elements.

2.2 Models of Pounding Force During Collision Between Structures

The second approach, which has been applied to model structural pounding during earthquakes, is to use directly the model of impact force during contact (force-based models). The experimental results (see Goland 1955; Goldsmith 1960;

Van Mier et al. 1991; Jankowski 2010) show that the impact force history depends substantially on a number of factors, such as masses of colliding structures, contact surface geometry, material properties, relative prior-impact velocity, structural material properties and even history of previous impacts.

The pounding force time history during impact consists of two phases (periods). The approach period starts at the beginning of contact and lasts till the peak deformation. It is followed by a restitution period which is finished at the moment of separation. The results of experiments indicate (see Goldsmith 1960; Jankowski 2010) that, at the beginning of the approach period, colliding elements are within the elastic range but, later on, plastic deformations, local cracking or crushing usually take place. On the other hand, the accumulated elastic strain energy is released without major plastic effects in the second phase of impact, i.e. during the restitution period. It has been observed that majority of the energy dissipated during impact is lost during the approach period of collision, while relatively small amount of energy is dissipated during the restitution period (Goldsmith 1960). Moreover, the experimental results show that during the approach period, a rapid increase in the pounding force is usually observed, whereas, during the restitution period, the force decreases with a lower rate, which is often reduced even further just before the separation (see Fig. 2.3a). It has also been observed that the relation between pounding force and deformation is non-linear with larger increase in values of pounding force for larger deformations (see Fig. 2.3b).

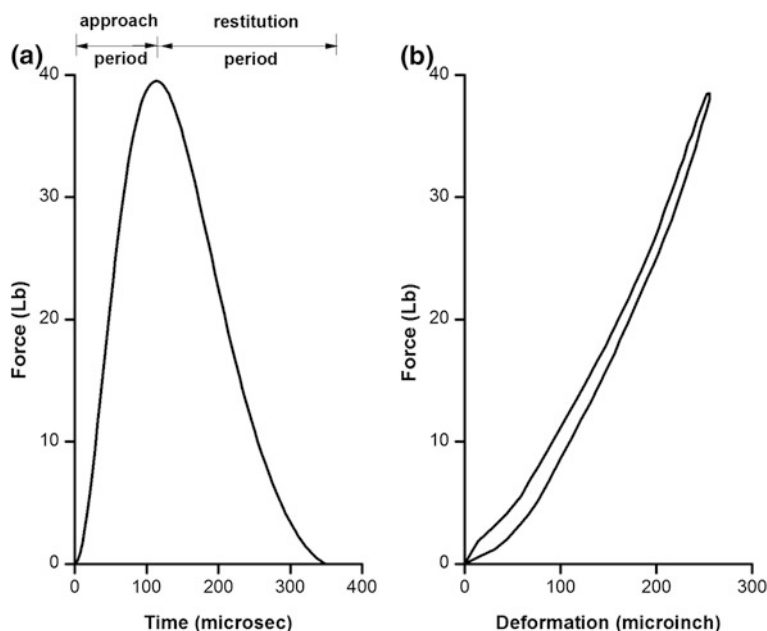
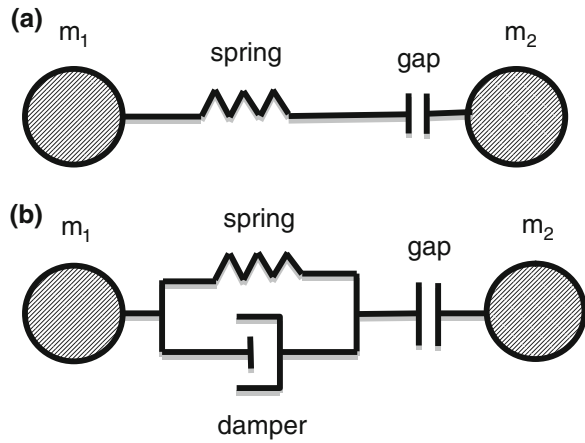


Fig. 2.3 Example of pounding force diagrams obtained from experiments: **a** pounding force time history; **b** relation between pounding force and deformation (after Crook 1952 and Goldsmith 1960)

Fig. 2.4 Equivalent force-based models of pounding: **a** with only spring; **b** with spring and damper



The pounding force between structures is usually simulated by the use of elastic or viscoelastic impact elements, which become active when contact starts, i.e. when the gap between elements is reduced to zero (see Fig. 2.4). Several types of such elements have been employed by researchers to model the phenomenon.

2.2.1 Linear Elastic Model

The basic impact element consists of a simple linear elastic spring (see Maison and Kasai 1990, 1992; Filiatrault et al. 1995; Zanardo et al. 2002; Kim and Shinozuka 2003; Karayannis and Favvata 2005). The pounding force during impact, $F(t)$, for this model is expressed as:

$$F(t) = k\delta(t) \quad (2.5)$$

where $\delta(t)$ is the deformation of colliding structural elements and k denotes the impact element's stiffness which accounts for the local stiffness at the contact location. The major drawback of the linear elastic model is that it does not account for the energy dissipation during collision.

2.2.2 Linear Viscoelastic Model

The lack of energy dissipation properties is overcome in the linear viscoelastic model (Kelvin-Voigt model), in which the impact element consists of a linear spring with addition of linear damper (Wolf and Skrikerud 1980; Anagnostopoulos 1988, 1995, 1996; Anagnostopoulos and Spiliopoulos 1992; Jankowski et al. 1998; Zhu et al. 2002; Pekau and Zhu 2006; Komodromos et al. 2007; Polycarpou and

Komodromos 2010). The pounding force during impact, $F(t)$, for the linear viscoelastic model is expressed as:

$$F(t) = k\delta(t) + c\dot{\delta}(t) \quad (2.6)$$

where $\dot{\delta}(t)$ describes the relative velocity between colliding structural elements and c is the impact element's damping, which can be calculated based on the formula (Anagnostopoulos 1988, 2004):

$$c = 2\zeta \sqrt{k \frac{m_1 m_2}{m_1 + m_2}} \quad (2.7)$$

in which ζ denotes the damping ratio related to the coefficient of restitution, e , by the following relation (Anagnostopoulos 2004):

$$\zeta = \frac{-\ln e}{\sqrt{\pi^2 + (\ln e)^2}} \quad (2.8)$$

A shortcoming of the linear spring-damper element is a negative impact force observed just before separation which does not have a physical explanation (Goldsmith 1960; Hunt and Crossley 1975; Marhefka and Orin 1999). This effect is related to the fact that the viscous component is active during the whole time of the restitution period [see Eq. (2.6)]. Moreover, the activation of the viscous component with the same damping coefficient during the approach and restitution period results in a uniform dissipation of energy during the whole time of collision, which is also not fully consistent with the reality (Goldsmith 1960; Valles and Reinhorn 1996, 1997). As described before, most of the energy is lost during the approach period and in the second phase of impact, i.e. in the restitution period, the accumulated elastic strain energy is released with only minor energy dissipation. Nevertheless, due to its simplicity, the linear viscoelastic model has been widely and successfully used in a number of analyses of earthquake-induced structural pounding.

2.2.3 Modified Linear Viscoelastic Model

In order to eliminate the sticky tensile force that appears just before separation of colliding structures in the case of the linear viscoelastic model, a modified version of the model, in which the damping term is activated only during the approach period of collision, was proposed (Mahmoud and Jankowski 2011). The pounding force during impact, $F(t)$, for this model is defined as:

$$\begin{aligned} F(t) &= k\delta(t) + c\dot{\delta}(t) && \text{for } \dot{\delta}(t) > 0 \text{ (approach period)} \\ F(t) &= k\delta(t) && \text{for } \dot{\delta}(t) \leq 0 \text{ (restitution period)} \end{aligned} \quad (2.9)$$

where the impact element's damping, c , is defined by Eq. (2.7). However, the relation between the impact damping ratio and the coefficient of restitution from Eq. (2.8) is no longer valid and, in order to satisfy the relation between the post-impact and the prior-impact relative velocities [see Eq. (2.2)], the following relation has been determined (see Mahmoud and Jankowski 2011):

$$\zeta = \frac{1 - e^2}{e(\pi - 2) + 2} \quad (2.10)$$

2.2.4 Hertz Non-linear Elastic Model

In order to model the pounding force-deformation relation more realistically (see Fig. 2.3b), a non-linear elastic spring following the Hertz law of contact (Hertz 1882) has been used in a number of studies (Jing and Young 1991; Davis 1992; Pantelides and Ma 1998; Chau and Wei 2001). The pounding force during impact, $F(t)$, for the Hertz non-linear elastic model is expressed as:

$$F(t) = \beta \delta^{\frac{3}{2}}(t) \quad (2.11)$$

where β is the impact stiffness parameter which depends on material properties and geometry of colliding bodies. A wide range of impact stiffness parameters for collisions between concrete elements has been determined by Van Mier et al. (1991) based on the results of experiments. It has been verified that the impact stiffness parameters for steel-to-steel collisions take even higher values (Goldsmith 1960; Chau et al. 2003). Goldsmith (1960) described simplified formulae to calculate the impact stiffness parameters for certain shapes of colliding bodies. For example, the impact stiffness parameter for collisions between two spheres can be calculated as:

$$\beta = \frac{4}{3\pi(h_1 + h_2)} \sqrt{\frac{R_1 R_2}{R_1 + R_2}} \quad (2.12)$$

where R_i , ($i = 1, 2$) is a radius of the colliding body with mass m_i , and h_i is defined as (Goldsmith 1960):

$$h_i = \frac{1 - \nu_i^2}{\pi E_i} \quad (2.13)$$

where ν_i stands for the Poisson's ratio and E_i denotes the Young's modulus of the material. When $R_2 \rightarrow \infty$, i.e. when the second body becomes a massive plane surface, the impact stiffness parameter, β , is defined as (Goldsmith 1960):

$$\beta = \frac{4}{3\pi(h_1 + h_2)} \sqrt{R_1} \quad (2.14)$$

The disadvantage of the Hertz contact law model is that it is fully elastic and does not account for the energy dissipation during contact due to plastic deformations, local cracking, friction, etc.

2.2.5 Hertzdamp Non-linear Model

Although the non-linear Hertz model effectively captures the relation between pounding force and deformation, its drawback, related to the fact that it does not account for the dissipated energy during collisions, causes serious problems. Therefore, the Hertzdamp model was considered to study the pounding phenomenon in the field of earthquake engineering (see Muthukumar and DesRoches 2006; Ye et al. 2009). The energy loss during impact is taken into account by adding non-linear damping to the Hertz model (see Lankarani and Nikraves 1990, 1994). The pounding force during impact, $F(t)$, for the Hertzdamp non-linear model is expressed as (Lankarani and Nikraves 1990, 1994; Muthukumar and DesRoches 2006):

$$F(t) = \beta \dot{\delta}^3(t) \left[1 + \frac{3(1 - e^2)}{4(\dot{x}_1^0 - \dot{x}_2^0)} \dot{\delta}(t) \right] \quad (2.15)$$

2.2.6 Non-linear Viscoelastic Model

Disadvantage of the non-linear Hertz model is also overcome in the non-linear viscoelastic model (see Jankowski 2005a, b, 2006b, 2007a, 2008; Mahmoud and Jankowski 2009, 2010; Mahmoud et al. 2012, 2013; Sołtysik and Jankowski 2013), in which the non-linear spring, following the Hertz law of contact, is applied together with the non-linear damper activated during the approach period of collision. This approach allows us to simulate more accurately the process of energy dissipation, which takes place mainly during that period (Goldsmith 1960). The pounding force during impact, $F(t)$, for the non-linear viscoelastic model is expressed as (Jankowski 2005b):

$$\begin{aligned} F(t) &= \bar{\beta} \dot{\delta}^3(t) + \bar{c}(t) \dot{\delta}(t) & \text{for } \dot{\delta}(t) > 0 \text{ (approach period)} \\ F(t) &= \bar{\beta} \dot{\delta}^3(t) & \text{for } \dot{\delta}(t) \leq 0 \text{ (restitution period)} \end{aligned} \quad (2.16)$$

where $\bar{\beta}$ is the impact stiffness parameter and $\bar{c}(t)$ is the impact element's damping, which can be obtained from the formula (Jankowski 2005b):

$$\bar{c}(t) = 2\bar{\xi}\sqrt{\bar{\beta}\sqrt{\delta(t)}\frac{m_1m_2}{m_1+m_2}} \quad (2.17)$$

where $\bar{\xi}$ denotes the damping ratio related to the coefficient of restitution, e (Jankowski 2006a):

$$\bar{\xi} = \frac{9\sqrt{5}}{2} \frac{1 - e^2}{e(e(9\pi - 16) + 16)} \quad (2.18)$$

2.3 Experimental Verification of the Effectiveness of Pounding Force Models

For the purposes of verification the accuracy of different models of structural pounding, the results of the numerical analyses have been compared with the results of the experimental studies conducted for various types of colliding elements (see also Jankowski 2005b; Mahmoud et al. 2008). The values of the impact stiffness parameters: k , β and $\bar{\beta}$, defining the models used in the numerical analysis, have been determined through iterative procedure so as to equalize the peak pounding force determined from the simulations with the peak pounding force obtained from the experiment. The difference between the experimental results and the results from the numerical analysis has been assessed by calculating the normalized root mean square (RMS) error (see Bendat and Piersol 1971):

$$RMSE = \frac{\sqrt{\sum_{i=1}^{NV} (H_i - \bar{H}_i)^2}}{\sqrt{\sum_{i=1}^{NV} H_i^2}} \cdot 100\% \quad (2.19)$$

where H_i , \bar{H}_i are the values from the time history record obtained from the experiment and from the numerical analysis, respectively; and NV denotes a number of values in these history records. In the numerical analysis concerning examples presented in this chapter, the time-stepping Newmark method (Newmark 1959), with the standard parameters: $\gamma_N = 0.5$ and $\beta_N = 0.25$ assuring the stability and accuracy of the results (see Bathe 1982; Chopra 1995), has been applied to determine the structural response.

2.3.1 Impact Between a Ball Falling Onto a Rigid Surface

In this section, the results of the numerical analysis are compared with the results of impact experiment conducted by dropping steel, concrete and timber balls of different masses onto a rigid surface (compare also Jankowski 2010). Balls have been

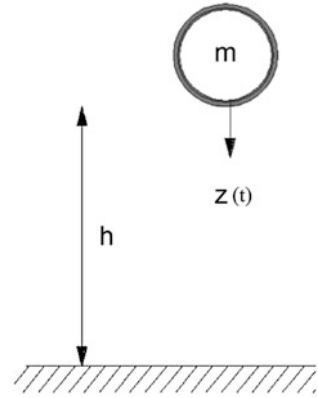
Table 2.1 Properties of balls used in the impact experiment

Material	Ball diameter (mm)	Ball mass (kg)
Steel (type 18G2A)	21	0.053–0.054
	50	0.538–0.541
	83	2.013
Concrete (grade C30/37)	103	1.329–1.350
	114	1.763–1.835
	128	2.531–2.636
Timber (pinewood)	55	0.065–0.066
	71	0.109–0.112
	118	0.493–0.497

dropped from various height levels in order to obtain different impact velocities. The properties of balls used in the experiment are specified in Table 2.1. B&K type 4344 accelerometer attached to the ball was used to measure the force time histories during impacts. System PULSE was applied for measuring and data acquisition purposes. The experimental setup is shown in Fig. 2.5.

**Fig. 2.5** Setup of the impact experiment

Fig. 2.6 Model of a ball falling onto a rigid surface



In the numerical analysis, the model of a ball falling onto a rigid surface, shown in Fig. 2.6, has been used. The dynamic equation of motion for such a model can be expressed as (Jankowski 2005b):

$$m\ddot{z}(t) + F(t) = mg \quad (2.20)$$

where m is mass of a ball, $\ddot{z}(t)$ its vertical acceleration, g stands for the acceleration of gravity and $F(t)$ is the pounding force, which is equal to zero when $z(t) \leq h$ (h is a drop height) and is defined by Eqs. (2.5), (2.6), (2.9), (2.11), (2.15) and (2.16) when $z(t) > h$, where deformation $\delta(t)$ is expressed as:

$$\delta(t) = z(t) - h \quad (2.21)$$

2.3.1.1 Impact Between Steel Elements

In the first example, the results of the numerical analysis are compared with the results of the experiment conducted for a steel ball of mass 2.013 kg impacting the steel surface with the velocity of 0.92 m/s. The following values of parameters defining different pounding force models have been used in the numerical analysis: $k = 3.45 \times 10^8$ N/m for the linear elastic model, $k = 4.82 \times 10^8$ N/m, $\xi = 0.17$ ($e = 0.58$) for the linear viscoelastic model, $k = 5.03 \times 10^8$ N/m, $\xi = 0.43$ ($e = 0.58$) for the modified linear viscoelastic model, $\beta = 2.94 \times 10^{10}$ N/m^{3/2} for the Hertz non-linear elastic model, $\beta = 3.76 \times 10^{10}$ N/m^{3/2}, $e = 0.58$ for the Hertz-damp non-linear model and $\bar{\beta} = 6.60 \times 10^{10}$ N/m^{3/2}, $\bar{\xi} = 0.49$ ($e = 0.58$) for the non-linear viscoelastic model. The time-stepping Newmark method with constant time step $\Delta t = 1 \times 10^{-6}$ s has been used to solve the equation of motion (2.20) numerically. The pounding force time history measured during the experiment and the histories received from the numerical analysis, for the considered example of

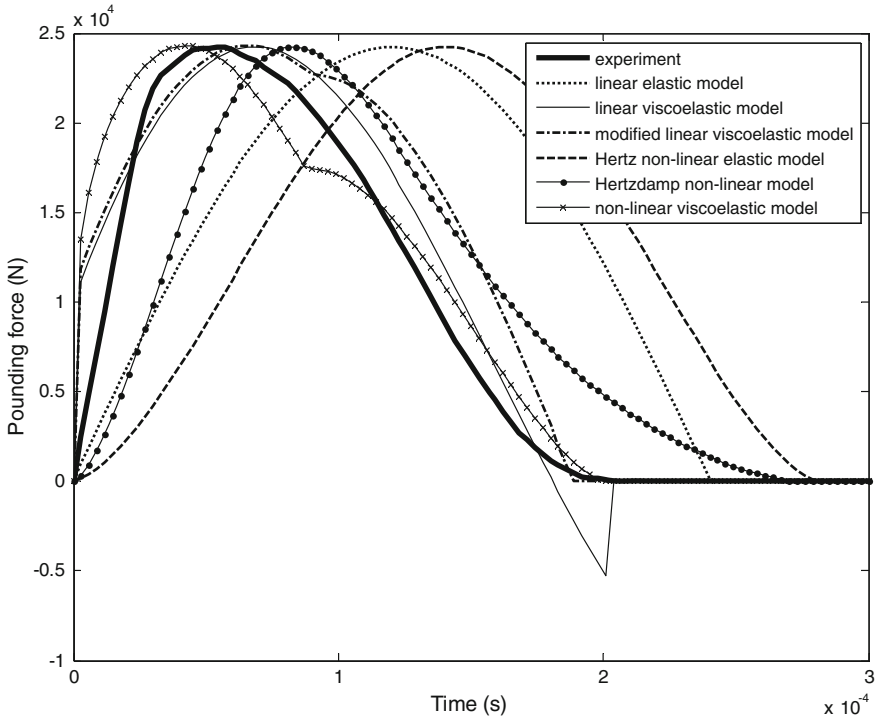


Fig. 2.7 Pounding force time histories for impact between steel elements

impact between steel elements, are presented in Fig. 2.7. Using Eq. (2.19), the RMS errors for pounding force histories have been calculated as equal to: 72.3 % for the linear elastic model, 18.6 % for the linear viscoelastic model, 26.5 % for the modified linear viscoelastic model, 93.1 % for the Hertz non-linear elastic model, 39.1 % for the Hertz damp non-linear model and 21.9 % for the non-linear viscoelastic model.

2.3.1.2 Impact Between Concrete Elements

The second example concerns the comparison between the results of the numerical simulations and the experiment conducted for a concrete ball of mass 1.763 kg impacting the concrete surface with the velocity of 0.13 m/s. In the numerical analysis, the following values of parameters, defining different pounding force models, have been used: $k = 4.33 \times 10^7$ N/m for the linear elastic model, $k = 4.91 \times 10^7$ N/m, $\xi = 0.09$ ($e = 0.76$) for the linear viscoelastic model, $k = 5.47 \times 10^7$ N/m, $\xi = 0.19$ ($e = 0.76$) for the modified linear viscoelastic model, $\beta = 5.92 \times 10^9$ N/m^{3/2} for the Hertz non-linear elastic model, $\beta = 6.39 \times 10^9$ N/m^{3/2}, $e = 0.76$ for the

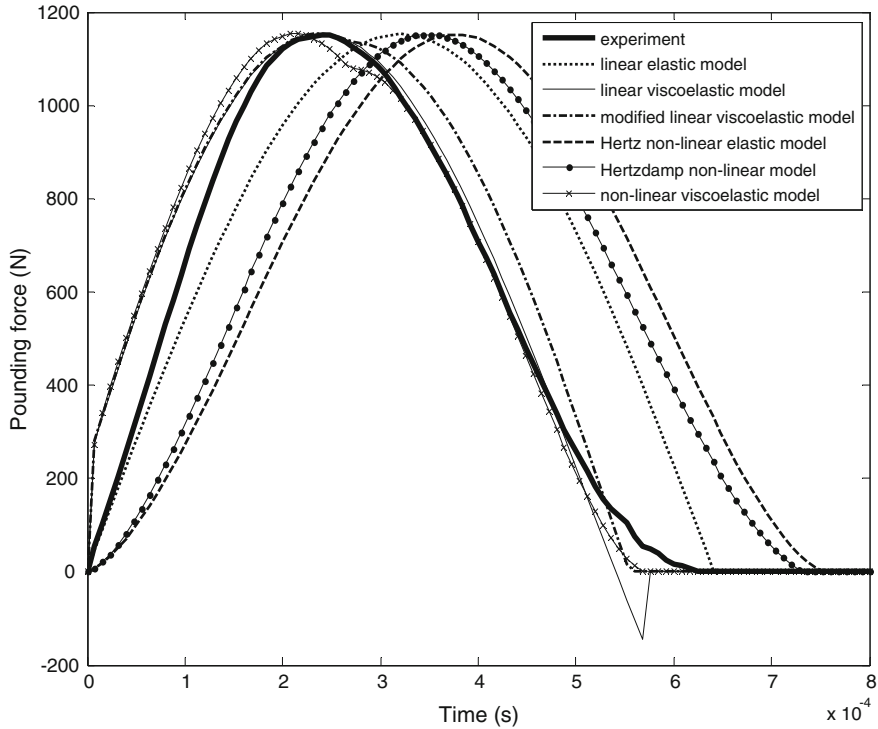


Fig. 2.8 Pounding force time histories for impact between concrete elements

Hertz damp non-linear model and $\bar{p} = 1.02 \times 10^{10} \text{ N/m}^{3/2}$, $\bar{\xi} = 0.22$ ($e = 0.76$) for the non-linear viscoelastic model. The time-stepping Newmark method with constant time step $\Delta t = 1 \times 10^{-5} \text{ s}$ has been used to solve the equation of motion (2.20) numerically. The pounding force time history measured during the experiment and the histories received from the numerical analysis, for the considered example of impact between concrete elements, are presented in Fig. 2.8. The RMS errors for these pounding force time histories have been calculated as equal to: 36.1 % for the linear elastic model, 12.7 % for the linear viscoelastic model, 15.7 % for the modified linear viscoelastic model, 59.3 % for the Hertz non-linear elastic model, 49.4 % for the Hertz damp non-linear model and 11.9 % for the non-linear viscoelastic model.

2.3.1.3 Impact Between Timber Elements

In the third example, the results of the numerical analysis are compared with the results of the experiment conducted for a timber ball of mass 0.109 kg impacting the timber surface with the velocity of 0.39 m/s. The following values of parameters, defining different pounding force models, have been used in the numerical

analysis: $k = 1.83 \times 10^6$ N/m for the linear elastic model, $k = 2.28 \times 10^6$ N/m, $\xi = 0.16$ ($e = 0.61$) for the linear viscoelastic model, $k = 2.62 \times 10^6$ N/m, $\xi = 0.38$ ($e = 0.61$) for the modified linear viscoelastic model, $\beta = 1.33 \times 10^8$ N/m^{3/2} for the Hertz non-linear elastic model, $\beta = 1.66 \times 10^8$ N/m^{3/2}, $e = 0.61$ for the Hertzdamp non-linear model and $\bar{\beta} = 3.11 \times 10^8$ N/m^{3/2}, $\bar{\xi} = 0.43$ ($e = 0.61$) for the non-linear viscoelastic model. The time-stepping Newmark method with constant time step $\Delta t = 1 \times 10^{-5}$ s has been used to solve the equation of motion (2.20) numerically. The pounding force time history measured during the experiment and the histories received from the numerical analysis, for the considered example of impact between timber elements, are presented in Fig. 2.9. Using Eq. (2.19), the RMS errors for pounding force histories have been calculated as equal to: 64.3 % for the linear elastic model, 20.7 % for the linear viscoelastic model, 26.6 % for the modified linear viscoelastic model, 85.8 % for the Hertz non-linear elastic model, 53.6 % for the Hertzdamp non-linear model and 20.8 % for the non-linear viscoelastic model.

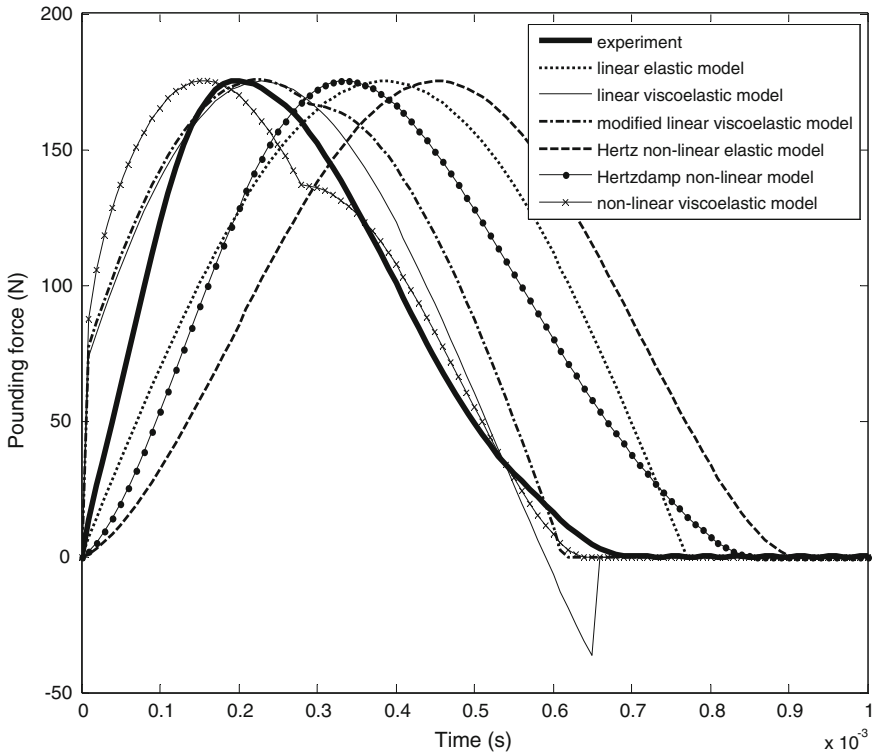


Fig. 2.9 Pounding force time histories for impact between timber elements



Fig. 2.10 Setup of the shaking table experiment

2.3.2 Pounding Between Models of Tower Structures

In this section, the results of the numerical analysis are compared with the results of the shaking table experiment focused on pounding between two tower models with different impacting materials (compare also Jankowski 2007b, 2010). Two 1 m high tower models (see Fig. 2.10) with different dynamic properties were built to be tested during the experiment. The columns were arranged in a rectangular pattern with a spacing of 0.22 m along the shaking direction (longitudinal one) and a spacing of 0.3 m along the orthogonal (transverse) direction (compare also Falborski and Jankowski 2013). All supporting elements used in the left tower model had a rectangular cross section with dimensions: 6×6 mm, whereas the model of the right tower was constructed of members with a section of 8×8 mm. The total mass of the supporting columns with horizontal connections and additional bracings was equal to $m_{c1} = 2.258$ kg for the left tower model and $m_{c2} = 3.864$ kg for the right one. Elements of external dimensions $0.25 \times 0.25 \times 0.05$ m made of different building materials, i.e. steel, concrete and timber (see Figs. 2.11 and 2.12), were fixed at the top of each tower. With the help of additional masses in the form of plates and bolts (see Figs. 2.11 and 2.12), the top mass of the tower models was kept constant for all experimental tests, apart from the material used, and was equal to $m_{t1} = 9.485$ kg for the left tower model and $m_{t2} = 18.337$ kg for the right one. Based on the free



Fig. 2.11 Top view of the left tower with impacting elements (made of steel, concrete and timber) and additional masses



Fig. 2.12 Top view of the right tower with impacting elements (made of steel, concrete and timber) and additional masses

vibration tests, the following dynamic parameters have been determined for both tower models: $f_1 = 2.59$ Hz, $\xi_{s1} = 0.004$, $f_2 = 2.99$ Hz, $\xi_{s2} = 0.01$, where f_i , ξ_{si} ($i = 1, 2$) are the natural frequency and the structural damping ratio, respectively. The initial gap size of $d = 0.04$ m between the towers has been considered in the study. The tower models have been excited in the horizontal direction by the NS component of the El Centro earthquake (18.05.1940). Two ENDEVCO type 7752 accelerometers, which were attached to the tower models at their top (see Fig. 2.10), were used to measure the time histories during the ground motion.

In the numerical analysis, a model, in which both towers are simulated as SDOF systems, as shown in Fig. 2.13, has been used. The dynamic equation of motion for such a model can be written as (Jankowski 2005b):

$$\begin{aligned}
 & \begin{bmatrix} m_1 & 0 \\ 0 & m_2 \end{bmatrix} \begin{bmatrix} \ddot{x}_1(t) \\ \ddot{x}_2(t) \end{bmatrix} + \begin{bmatrix} C_1 & 0 \\ 0 & C_2 \end{bmatrix} \begin{bmatrix} \dot{x}_1(t) \\ \dot{x}_2(t) \end{bmatrix} \\
 & + \begin{bmatrix} K_1 & 0 \\ 0 & K_2 \end{bmatrix} \begin{bmatrix} x_1(t) \\ x_2(t) \end{bmatrix} + \begin{bmatrix} F(t) \\ -F(t) \end{bmatrix} = - \begin{bmatrix} m_1 & 0 \\ 0 & m_2 \end{bmatrix} \begin{bmatrix} \ddot{x}_g(t) \\ \ddot{x}_g(t) \end{bmatrix}
 \end{aligned} \tag{2.22}$$

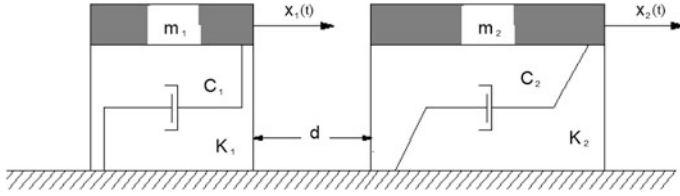


Fig. 2.13 Model of two colliding SDOF systems

where $x_i(t)$, $\dot{x}_i(t)$, $\ddot{x}_i(t)$ are the horizontal displacement, velocity and acceleration of tower i ($i = 1, 2$), respectively, $K_i = 4\pi^2 f_i^2 m_i$, $C_i = 2\zeta_{Si} \sqrt{K_i m_i}$ denote stiffness and damping coefficients, $\ddot{x}_g(t)$ stands for the acceleration of input ground motion and $F(t)$ is the pounding force, which is equal to zero when $\delta(t) \leq 0$ and is defined by Eqs. (2.5), (2.6), (2.9), (2.11), (2.15) and (2.16) if $\delta(t) > 0$, where deformation $\delta(t)$ is defined as:

$$\delta(t) = x_1(t) - x_2(t) - d \quad (2.23)$$

The following mass values: $m_1 = 10.004$ kg, $m_2 = 19.226$ kg have been applied in the numerical analysis, as calculated from the formula (Harris and Piersol 2002):

$$m_i = m_{fi} + 0.23m_{ci} \quad (i = 1, 2) \quad (2.24)$$

In order to solve the equation of motion (2.22) numerically, the time-stepping Newmark method with constant time step $\Delta t = 0.002$ s has been used.

2.3.2.1 Pounding Between Steel Elements

The first example shows a comparison between the results of the numerical analysis and the experiment conducted for pounding of tower models with impacting steel elements (steel type 18G2A). The following values of parameters of different pounding force models have been applied in the numerical analysis: $k = 5.67 \times 10^7$ N/m for the linear elastic model, $k = 7.93 \times 10^7$ N/m, $\xi = 0.12$ ($e = 0.68$) for the linear viscoelastic model, $k = 8.54 \times 10^7$ N/m, $e = 0.68$ for the modified linear viscoelastic model, $\beta = 3.94 \times 10^9$ N/m^{3/2} for the Hertz non-linear elastic model, $\beta = 5.14 \times 10^9$ N/m^{3/2}, $e = 0.68$ for the Hertz damp non-linear model and $\bar{\beta} = 8.32 \times 10^9$ N/m^{3/2}, $\bar{\xi} = 0.31$ ($e = 0.68$) for the non-linear viscoelastic model. The displacement time history of the left tower model (lighter and more flexible one) obtained from the experiment and the histories received from the numerical analysis are shown in Fig. 2.14. Using Eq. (2.19), the RMS errors for the time histories have been calculated as equal to: 28.7 % for the linear elastic model,

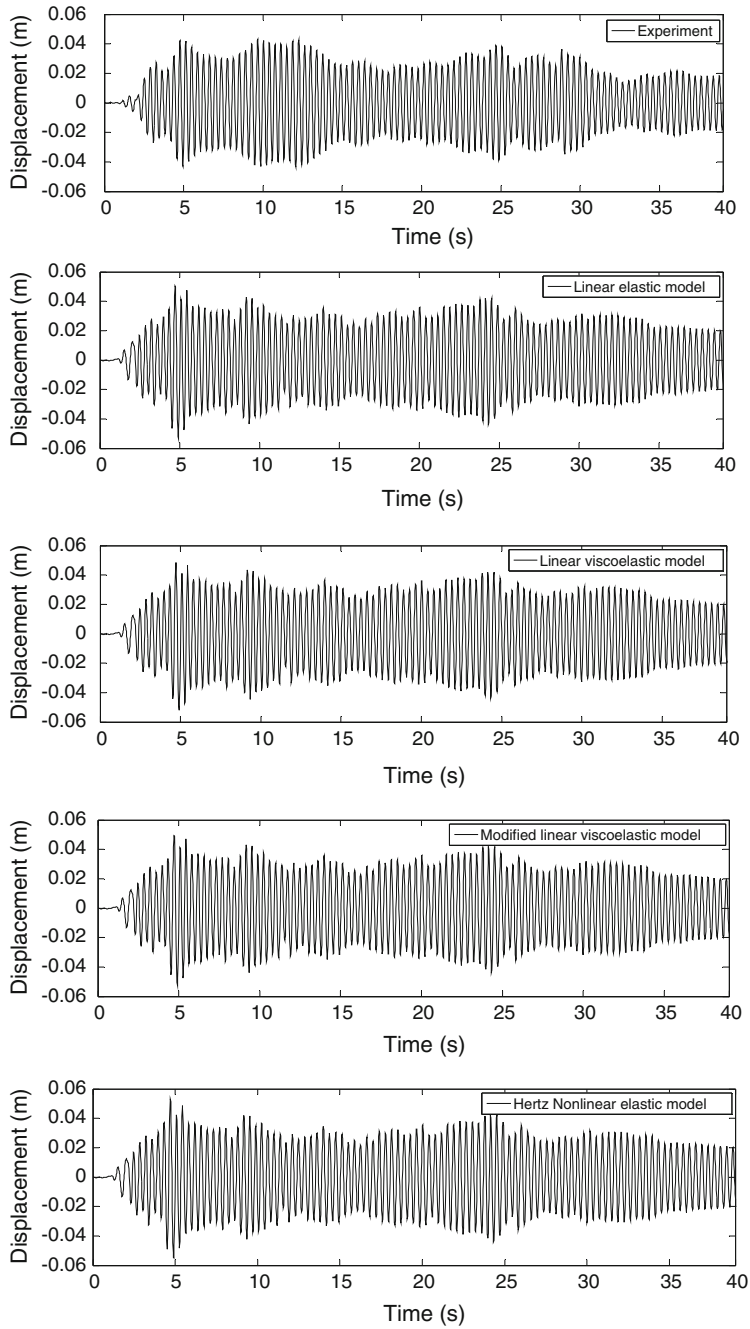


Fig. 2.14 Displacement time histories of the left tower model for pounding between steel elements under the El Centro earthquake

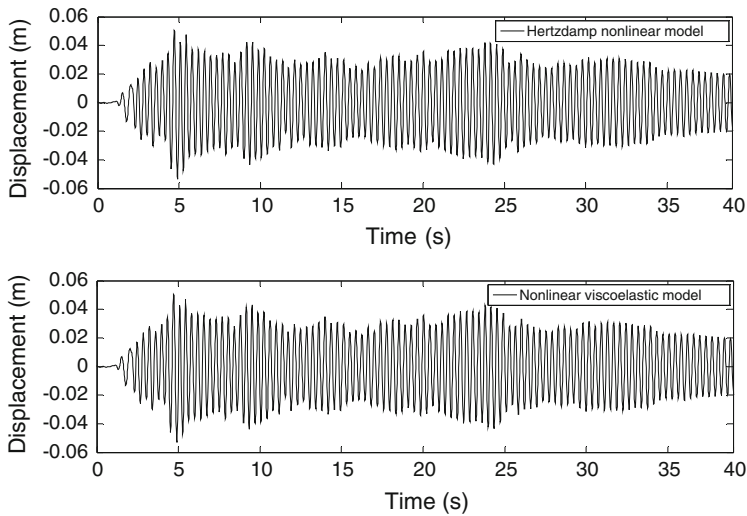


Fig. 2.14 (continued)

23.2 % for the linear viscoelastic model, 24.3 % for the modified linear viscoelastic model, 22.9 % for the Hertz non-linear elastic model, 22.5 % for the Hertz damp non-linear model and 22.6 % for the non-linear viscoelastic model.

2.3.2.2 Pounding Between Concrete Elements

In this example, the results of the numerical analysis are compared with the results of the experiment conducted for pounding of tower models with impacting concrete elements (concrete grade C30/37). In the numerical analysis, the following values of parameters, defining different pounding force models, have been used: $k = 1.87 \times 10^7$ N/m for the linear elastic model, $k = 2.05 \times 10^7$ N/m, $\xi = 0.14$ ($e = 0.65$) for the linear viscoelastic model, $k = 2.36 \times 10^7$ N/m, $e = 0.65$ for the modified linear viscoelastic model, $\beta = 9.75 \times 10^8$ N/m^{3/2} for the Hertz non-linear elastic model, $\beta = 1.17 \times 10^9$ N/m^{3/2}, $e = 0.65$ for the Hertz damp non-linear model and $\bar{\beta} = 2.53 \times 10^9$ N/m^{3/2}, $\bar{\xi} = 0.35$ ($e = 0.65$) for the non-linear viscoelastic model. The displacement time history of the left tower model obtained from the experiment and the histories received from the numerical analysis are shown in Fig. 2.15. The RMS errors for these time histories have been calculated using Eq. (2.19) as equal to: 22.6 % for the linear elastic model, 15.3 % for the linear viscoelastic model, 18.7 % for the modified linear viscoelastic model, 22.4 % for the Hertz non-linear elastic model, 16.3 % for the Hertz damp non-linear model and 14.8 % for the non-linear viscoelastic model.

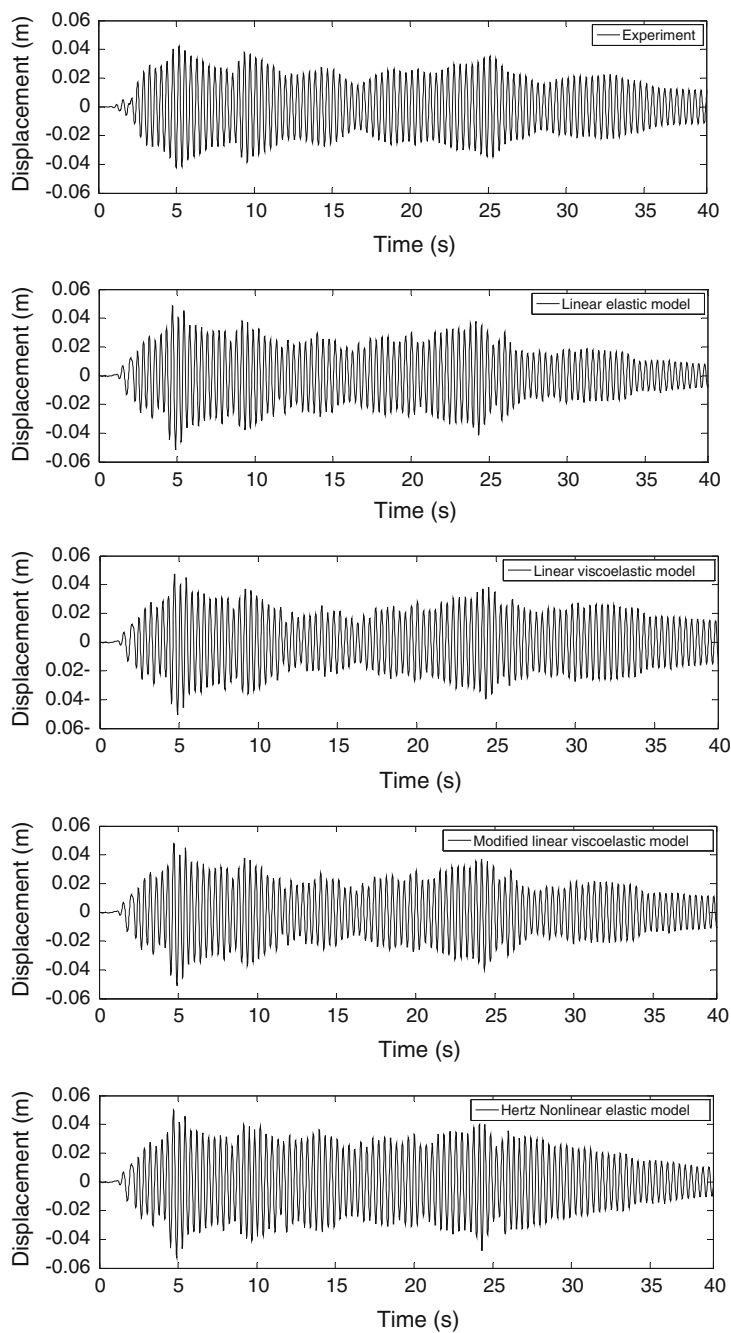


Fig. 2.15 Displacement time histories of the left tower model for pounding between concrete elements under the El Centro earthquake

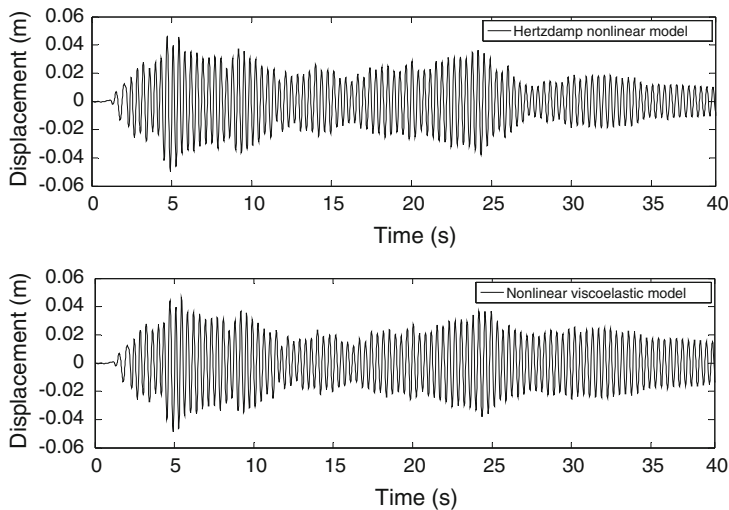


Fig. 2.15 (continued)

2.3.2.3 Pounding Between Timber Elements

The third example concerns a comparison between the results of the numerical analysis and the experiment conducted for pounding of tower models with impacting timber elements made of pinewood. The following values of parameters of different pounding force models have been applied in the numerical analysis: $k = 1.47 \times 10^6$ N/m for the linear elastic model, $k = 1.97 \times 10^6$ N/m, $\xi = 0.16$ ($e = 0.60$) for the linear viscoelastic model, $k = 2.33 \times 10^6$ N/m, $e = 0.60$ for the modified linear viscoelastic model, $\beta = 1.50 \times 10^8$ N/m^{3/2} for the Hertz non-linear elastic model, $\beta = 1.74 \times 10^8$ N/m^{3/2}, $e = 0.60$ for the Hertz damp non-linear model and $\bar{\beta} = 2.85 \times 10^8$ N/m^{3/2}, $\bar{\xi} = 0.44$ ($e = 0.60$) for the non-linear viscoelastic model. The displacement time history of the left tower model obtained from the experiment and the histories received from the numerical analysis are shown in Fig. 2.16. The RMS errors for these time histories have been calculated using Eq. (2.19) as equal to: 38.7 % for the linear elastic model, 25.2 % for the linear viscoelastic model, 27.6 % for the modified linear viscoelastic model, 43.8 % for the Hertz non-linear elastic model, 26.3 % for the Hertz damp non-linear model and 24.8 % for the non-linear viscoelastic model.

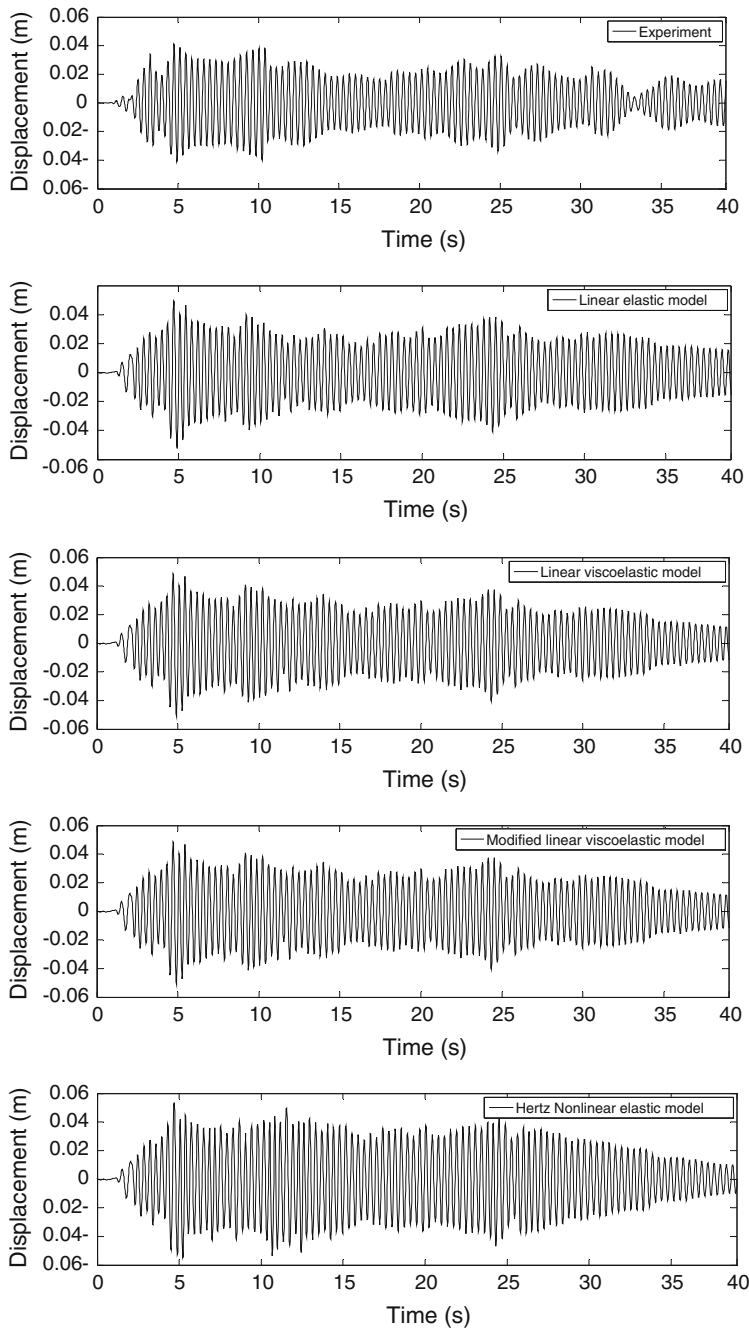


Fig. 2.16 Displacement time histories of the left tower model for pounding between timber elements under the El Centro earthquake

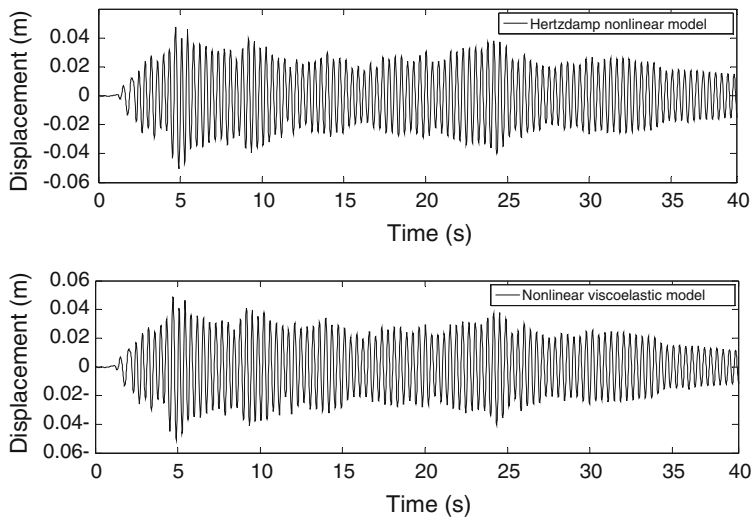


Fig. 2.16 (continued)

2.3.3 Conclusions

The results of the studies show that the linear viscoelastic and the non-linear viscoelastic models give the smallest errors in the pounding force time histories during single impact. In the case of the linear viscoelastic model, a negative impact force just before separation, which does not have a physical explanation, has been observed. However, the improvement introduced in the modified linear viscoelastic model, in order to overcome this drawback, does not really lead to the increase in the accuracy of the model.

Further analysis has shown that the application of the linear viscoelastic, the Hertz damp and the non-linear viscoelastic models results in the smallest errors in the response time histories of the analysed examples of structural pounding under earthquake excitation. The impact force models have been found to have some advantages and disadvantages when used for modelling of structural pounding. The results of the study indicate that the efficiency of them depends on the type of analysis conducted.

References

- Anagnostopoulos, S.A.: Pounding of buildings in series during earthquakes. *Earthquake Eng. Struct. Dynam.* **16**, 443–456 (1988)
- Anagnostopoulos S.A.: Earthquake induced pounding: state of the art. In: *Proceedings of 10th European Conference on Earthquake Engineering*, Vienna, Austria, 28 Aug–2 Sept 1994. pp. 897–905, Balkema, Rotterdam (1995)

- Anagnostopoulos, S.A.: Building pounding re-examined: how serious a problem is it? In: Eleventh World Conference on Earthquake Engineering, Acapulco, Mexico, Paper No. 2108, 23–28 June 1996
- Anagnostopoulos, S.A.: Equivalent viscous damping for modeling inelastic impacts in earthquake pounding problems. *Earthquake Eng. Struct. Dynam.* **33**, 897–902 (2004)
- Anagnostopoulos, S.A., Spiliopoulos, K.V.: An investigation of earthquake induced pounding between adjacent buildings. *Earthquake Eng. Struct. Dynam.* **21**, 289–302 (1992)
- Azevedo, J., Bento, R.: Design criteria for buildings subjected to pounding. In: Eleventh World Conference on Earthquake Engineering, Acapulco, Mexico, Paper No. 1063, 23–28 June 1996
- Bathe, K.J.: *Finite Element Procedures in Engineering Analysis*. Prentice-Hall, Englewood Cliffs (1982)
- Bendat, J.S., Piersol, A.G.: *Random Data: Analysis and Measurement Procedures*. Wiley, New York (1971)
- Chau, K.T., Wei, X.X.: Pounding of structures modelled as non-linear impacts of two oscillators. *Earthquake Eng. Struct. Dynam.* **30**, 633–651 (2001)
- Chau, K.T., Wei, X.X., Guo, X., Shen, C.Y.: Experimental and theoretical simulations of seismic poundings between two adjacent structures. *Earthquake Eng. Struct. Dynam.* **32**, 537–554 (2003)
- Chopra, A.K.: *Dynamics of Structures: Theory and Applications to Earthquake Engineering*. Prentice-Hall, Englewood Cliffs (1995)
- Crook, A.W.: A study on some impacts between metal bodies by a piezoelectric method. *Proc. Roy. Soc. A* **212**, 377–390 (1952)
- Davis, R.O.: Pounding of buildings modelled by an impact oscillator. *Earthquake Eng. Struct. Dynam.* **21**, 253–274 (1992)
- DesRoches, R., Muthukumar, S.: Effect of pounding and restrainers on seismic response of multiple-frame bridges. *J. Struct. Eng.* **128**, 860–869 (2002)
- Falborski, T., Jankowski, R.: Polymeric bearings—a new base isolation system to reduce structural damage during earthquakes. *Key Eng. Mater.* **569–570**, 143–150 (2013)
- Filiatrault, A., Wagner, P., Cherry, S.: Analytical prediction of experimental building pounding. *Earthquake Eng. Struct. Dynam.* **24**, 1131–1154 (1995)
- Goland, M., Wickersham, P.D., Dengler, M.A.: Propagation of elastic impact in beams in bending. *J. Appl. Mech.* **22**, 1–7 (1955)
- Goldsmith, W.: *Impact: The Theory and Physical Behaviour of Colliding Solids*. Edward Arnold, London (1960)
- Harris, C.M., Piersol, A.G.: *Harris' Shock and Vibration Handbook*. McGraw-Hill, New York (2002)
- Hertz, H.: Über die Berührung fester elastischer Körper (On the contact of elastic solids). *J. für die Reine und Angewandte Mathematik* **29**, 156–171 (1882). (in German)
- Hunt, K.H., Crossley, F.R.E.: Coefficient of restitution interpreted as damping in vibroimpact. *J. Appl. Mech. ASME* **42**, 440–445 (1975)
- Jankowski, R.: Impact force spectrum for damage assessment of earthquake-induced structural pounding. *Key Eng. Mater.* **293–294**, 711–718 (2005a)
- Jankowski, R.: Non-linear viscoelastic modelling of earthquake-induced structural pounding. *Earthquake Eng. Struct. Dynam.* **34**, 595–611 (2005b)
- Jankowski, R.: Analytical expression between the impact damping ratio and the coefficient of restitution in the non-linear viscoelastic model of structural pounding. *Earthquake Eng. Struct. Dynam.* **35**, 517–524 (2006a)
- Jankowski, R.: Pounding force response spectrum under earthquake excitation. *Eng. Struct.* **28**, 1149–1161 (2006b)
- Jankowski, R.: Assessment of damage due to earthquake-induced pounding between the main building and the stairway tower. *Key Eng. Mater.* **347**, 339–344 (2007a)
- Jankowski, R.: Non-linear analysis of pounding-involved response of equal height buildings under earthquake excitation. DSc dissertation, Wydawnictwo Politechniki Gdańskiej, Gdańsk, Poland (2007b)

- Jankowski, R.: Earthquake-induced pounding between equal height buildings with substantially different dynamic properties. *Eng. Struct.* **30**(10), 2818–2829 (2008)
- Jankowski, R.: Experimental study on earthquake-induced pounding between structural elements made of different building materials. *Earthquake Eng. Struct. Dynam.* **39**, 343–354 (2010)
- Jankowski, R., Wilde, K., Fujino, Y.: Pounding of superstructure segments in isolated elevated bridge during earthquakes. *Earthquake Eng. Struct. Dynam.* **27**, 487–502 (1998)
- Jing, H.-S., Young, M.: Impact interactions between two vibration systems under random excitation. *Earthquake Eng. Struct. Dynam.* **20**, 667–681 (1991)
- Karayannis, C.G., Favvata, M.J.: Earthquake-induced interaction between adjacent reinforced concrete structures with non-equal heights. *Earthquake Eng. Struct. Dynam.* **34**, 1–20 (2005)
- Kim, S.-H., Shinozuka, M.: Effects of seismically induced pounding at expansion joints of concrete bridges. *J. Eng. Mech.* **129**, 1225–1234 (2003)
- Komodromos, P., Polycarpou, P.C., Papaloizou, L., Phocas, M.C.: Response of seismically isolated buildings considering poundings. *Earthquake Eng. Struct. Dynam.* **36**, 1605–1622 (2007)
- Lankarani, H.M., Nikravesh, P.E.: A contact force model with hysteresis damping for impact analysis of multibody systems. *J. Mech. Design ASME* **112**, 369–376 (1990)
- Lankarani, H.M., Nikravesh, P.E.: Continuous contact force models for impact analysis in multibody systems. *Nonlinear Dyn.* **5**, 193–207 (1994)
- Leibovich, E., Rutenberg, A., Yankelevsky, D.Z.: On eccentric seismic pounding of symmetric buildings. *Earthquake Eng. Struct. Dynam.* **25**, 219–233 (1996)
- Mahmoud, S., Abd-Elhamed, A., Jankowski, R.: Earthquake-induced pounding between equal height multi-storey buildings considering soil-structure interaction. *Bull. Earthq. Eng.* **11**(4), 1021–1048 (2013)
- Mahmoud, S., Austrell, P.-E., Jankowski, R.: Simulation of the response of base-isolated buildings under earthquake excitations considering soil flexibility. *Earthq. Eng. Eng. Vibr.* **11**, 359–374 (2012)
- Mahmoud, S., Chen, X., Jankowski, R.: Structural pounding models with Hertz spring and nonlinear damper. *J. Appl. Sci.* **8**, 1850–1858 (2008)
- Mahmoud, S., Jankowski, R.: Elastic and inelastic multi-storey buildings under earthquake excitation with the effect of pounding. *J. Appl. Sci.* **9**(18), 3250–3262 (2009)
- Mahmoud, S., Jankowski, R.: Pounding-involved response of isolated and non-isolated buildings under earthquake excitation. *Earthq. Struct.* **1**(3), 231–252 (2010)
- Mahmoud, S., Jankowski, R.: Modified linear viscoelastic model of earthquake-induced structural pounding. *Iran. J. Sci. Technol.* **35**(C1), 51–62 (2011)
- Maison, B.F., Kasai, K.: Analysis for type of structural pounding. *J. Struct. Eng.* **116**, 957–977 (1990)
- Maison, B.F., Kasai, K.: Dynamics of pounding when two buildings collide. *Earthquake Eng. Struct. Dynam.* **21**, 771–786 (1992)
- Marhefka, D.W., Orin, D.E.: A compliant contact model with nonlinear damping for simulation of robotic systems. *IEEE Trans. Syst. Man Cyber. Part A Syst. Hum.* **29**, 566–572 (1999)
- Muthukumar, S., DesRoches, R.: A Hertz contact model with nonlinear damping for pounding simulation. *Earthquake Eng. Struct. Dynam.* **35**, 811–828 (2006)
- Newmark, N.: A method of computation for structural dynamics. *J. Eng. Mech. Div. ASCE* **85**, 67–94 (1959)
- Pantelides, C.P., Ma, X.: Linear and nonlinear pounding of structural systems. *Comput. Struct.* **66**, 79–92 (1998)
- Papadrakakis, M., Mouzakis, H., Plevris, N., Bitzarakis, S.A.: Lagrange multiplier solution method for pounding of buildings during earthquakes. *Earthquake Eng. Struct. Dynam.* **20**, 981–998 (1991)
- Pekau, O.A., Zhu, X.: Seismic behaviour of cracked concrete gravity dams. *Earthquake Eng. Struct. Dynam.* **35**, 477–495 (2006)
- Polycarpou, P.C., Komodromos, P.: On poundings of a seismically isolated building with adjacent structures during strong earthquakes. *Earthquake Eng. Struct. Dynam.* **39**, 933–940 (2010)

- Ruangrassamee, A., Kawashima, K.: Relative displacement response spectra with pounding effect. *Earthquake Eng. Struct. Dynam.* **30**, 1511–1538 (2001)
- Softysik, B., Jankowski, R.: Non-linear strain rate analysis of earthquake-induced pounding between steel buildings. *Int. J. Earth Sci. Eng.* **6**, 429–433 (2013)
- Van Mier, J.G.M., Puijssers, A.F., Reinhardt, H.W., Monnier, T.: Load-time response of colliding concrete bodies. *J. Struct. Eng.* **117**, 354–374 (1991)
- Valles, R.E., Reinhorn, A.M.: Evaluation, prevention and mitigation of pounding effects in building structures. In *Eleventh World Conference on Earthquake Engineering*, Acapulco, Mexico, Paper No. 26. 23–28 June 1996
- Valles, R.E., Reinhorn, A.M.: Evaluation, prevention and mitigation of pounding effects in building structures. Technical Report NCEER-97-0001. National Center for Earthquake Engineering Research, State University of New York, Buffalo, USA (1997)
- Wolf, J.P., Skrikerud, P.E.: Mutual pounding of adjacent structures during earthquakes. *Nucl. Eng. Des.* **57**, 253–275 (1980)
- Ye, K., Li, L., Zhu, H.: A note on the Hertz contact model with nonlinear damping for pounding simulation. *Earthquake Eng. Struct. Dynam.* **38**, 1135–1142 (2009)
- Zanardo, G., Hao, H., Modena, C.: Seismic response of multi-span simply supported bridges to a spatially varying earthquake ground motion. *Earthquake Eng. Struct. Dynam.* **31**, 1325–1345 (2002)
- Zhu, P., Abe, M., Fujino, Y.: Modelling three-dimensional non-linear seismic performance of elevated bridges with emphasis on pounding of girders. *Earthquake Eng. Struct. Dynam.* **31**, 1891–1913 (2002)

Earthquake-Induced Structural Pounding

Jankowski, R.; Mahmoud, S.

2015, XV, 156 p. 127 illus., 7 illus. in color., Hardcover

ISBN: 978-3-319-16323-9